

Supplementary Materials

Understanding the phase separation characteristics of nucleocapsid protein provides a new therapeutic opportunity against SARS-CoV-2

Dan Zhao^{1,10}, Weifan Xu^{2,10}, Xiaofan Zhang^{1,10}, Xiaoting Wang³, Yiyue Ge⁴, Enming Yuan¹, Yuanpeng Xiong⁵, Shenyang Wu⁶, Shuya Li¹, Nian Wu¹, Tingzhong Tian¹, Xiaolong Feng⁷, Hantao Shu¹, Peng Lang¹, Jingxin Li⁴, Fengcai Zhu^{4,8}, Xiaokun Shen⁹, Haitao Li¹⁰, Pulong Li^{2,*} and Jianyang Zeng^{1,11,*}

¹Institute for Interdisciplinary Information Sciences, Tsinghua University, Beijing, China.

²Beijing Advanced Innovation Center for Structural Biology, Beijing Frontier Research Center for Biological Structure, Tsinghua University-Peking University Joint Center for Life Sciences, School of Life Sciences, Tsinghua University, Beijing, China.

³Silexon AI Technology Co., Ltd., Nanjing, Jiangsu Province, China.

⁴NHC Key laboratory of Enteric Pathogenic Microbiology, Jiangsu Provincial Center for Diseases Control and Prevention, Nanjing, Jiangsu Province, 210009, China.

⁵Bioinformatics Division, BNRIST/Department of Computer Science and Technology, Tsinghua University, Beijing, China

⁶Protein Preparation and Identification Facility, Technology Center for Protein Science, Tsinghua University, Beijing, China.

⁷Institute of Pathology, Tongji Hospital, Tongji Medical College, Huazhong University of Science and Technology, Wuhan, Hubei Province, China.

⁸Center for Global Health, Nanjing Medical University, Nanjing, Jiangsu Province, 210009, China.

⁹Convalife (Shanghai) Co., Ltd., Shanghai, China.

¹⁰MOE Key Laboratory of Protein Sciences, Beijing Advanced Innovation Center for Structural Biology, Beijing Frontier Research Center for Biological Structure, Tsinghua-Peking Joint Center for Life Sciences, Department of Basic Medical Sciences, School of Medicine, Tsinghua University, Beijing 100084, China.

¹¹MOE Key Laboratory of Bioinformatics, Tsinghua University, Beijing, China.

¹⁰These authors contributed equally: Dan Zhao, Weifan Xu, Xiaofan Zhang.

*E-mail: pulongli@mail.tsinghua.edu.cn; zengjy321@tsinghua.edu.cn.

33 **Materials and Methods**

34 **Cell culture and transfection**

35 Vero E6 cells were kindly provided by Dr. Yiyue Ge and Dr. Jingxin Li from NHC
36 Key Laboratory of Enteric Pathogenic Microbiology, Jiangsu Provincial Center for
37 Disease Control and Prevention. Vero E6 cells were cultured in Dulbecco's modified
38 Eagle's medium (HyClone) supplemented with 10% fetal bovine serum (HyClone
39 SH30071.03 and SH30396.03) and maintained at 37°C in a humidified incubator with
40 5% CO₂. FuGENE 6 (Promega, E2691) was used for transient transfection according
41 to the manufacturer's instructions. The SARS-CoV-2 virus strain used in this study
42 was BetaCoV/JS03/human/2020 (EPI ISL 411953), which was isolated from a 40-
43 year old female confirmed as a COVID-19 case in December 2019. Vero E6 cells
44 were used to propagate the virus, and the viral titer was measured by the 50% tissue
45 culture infective dose (TCID₅₀) through microscopic observation of cytopathic effect.
46 All the SARS-CoV-2 infection related experiments were performed in a biosafety
47 level-3 (BLS-3) laboratory in Jiangsu Provincial Center for Diseases Control and
48 Prevention, Jiangsu, China.

49 **Construction of recombinant plasmids**

50 The recombinant plasmids of pET28a-N and pET22b-nsp12 were kindly provided by
51 Cellregen Co., Ltd. and Prof. Zhiyong Lou (Gao et al., 2020), respectively. The
52 mutants of pET28a-N were constructed by seamless cloning kits (Beyotime,
53 D7010M) and confirmed by sequencing. For the construction of mEGFP-N plasmids,
54 the full-length gene and truncations of SARS-CoV-2 N were both cloned into a
55 PL118 vector (an in-house modified vector based on pRSFDuet1) containing an N-
56 terminal 6×his-mEGFP tag, respectively. The full-length gene of SARS-CoV-2 N was
57 cloned into a pCDNA3.1 vector containing an N-terminal mCherry tag. The full-
58 length gene of SARS-CoV-2-Nsp12 was cloned into a pCDNA3.1 vector containing
59 an N-terminal GFP tag. The Ub11 domain of SARS-CoV-2 nsp3 (1-112 aa) was

60 cloned into a pGEX-4T-2 vector. The detailed primer sequences are listed in
61 Supplementary Table S1.

62

63 **Protein expression and purification**

64 The recombinant full-length mEGFP-N protein and truncations were overexpressed in
65 *E. coli* BL21 (DE3). After overnight induction by 0.2mM isopropyl β -D-
66 thiogalactoside (IPTG) at 16 °C in LB medium, cells were harvested and suspended in
67 the buffer (40mM HEPES, pH 7.5, 1M NaCl, 20mM imidazole and 2mM
68 phenylmethylsulfonyl fluoride). After cell lysis and centrifugation, the recombined
69 proteins were purified to homogeneity over HisTrap column and eluted with a linear
70 imidazole gradient from 20 mM to 500 mM. The proteins were further purified by
71 size-exclusion chromatography using a Superdex 200 Increase 10/300 GL column
72 (GE Healthcare) in elution buffer (40 mM HEPES, pH7.5, 1M NaCl, 5% glycerol, 1
73 mM EGTA, 1 mM MgCl₂). The purification procedures of the recombinant wild-type
74 pET28a-N protein and mutants were essentially the same as that of the mEGFP-N
75 protein except for a different size-exclusion chromatography buffer (20mM Tris, pH
76 7.5, 300mM NaCl).

77 The Ubl1 domain of nsp3 gene (1-112 aa) of SARS-CoV-2 was cloned into a
78 modified pGEX-4T-2 vector, with a GST tag. The plasmids were transformed into *E.*
79 *coli* BL21 (DE3). After overnight induction by 0.2mM IPTG at 16 °C in LB medium,
80 the cells were harvested and resuspended in lysis buffer (20 mM Tris-HCl, pH 7.5,
81 500 mM NaCl, 20mM Imidazole) and homogenized with an Emulsiflex C3 (Avestin)
82 high-pressure homogenizer at 4 °C. After centrifugation at 13,000 rpm, the
83 supernatant was loaded on a GST column and the fusion protein was directly digested
84 on the column overnight by the Thrombin protease (Beijing Solarbio Science &
85 Technology, T8021). The resultant protein was further loaded on a Superdex 75
86 10/300 Increase column (GE Healthcare, USA) in a buffer containing 40 mM HEPES,

87 pH 7.5, 1mM EGTA, 150 mM NaCl, 1 mM MgCl₂ and 5% glycerol. The purified
88 Ubl1 domain of nsp3 was concentrated and stored at -80 °C.

89

90 **Assembly of RdRp complex *in vitro***

91 The purification and assembly of RdRp complex of SARS-CoV-2 were essentially the
92 same as described previously (Gao et al., 2020) with minor modifications. Briefly, the
93 nsp12 gene was cloned into a modified pET22a vector, with the C-terminus
94 possessing a 10 × His-tag. The plasmids were transformed into *E. coli* BL21 (DE3),
95 and after overnight induction by 0.2mM IPTG at 16 °C in LB medium, cells were
96 harvested and suspended in the buffer (20 mM Tris-HCl, pH 7.5, 500 mM NaCl,
97 20mM Imidazole) and homogenized with an Emulsiflex C3 (Avestin) high-pressure
98 homogenizer at 4 °C. After centrifugation at 13,000 rpm, the supernatant was loaded
99 on Ni-NTA column (GE Healthcare, USA) and then further purified by a Hitrap Q
100 ion-exchange column (GE Healthcare, USA). The peaks eluted were loaded on a
101 Superdex 200 10/300 Increase column (GE Healthcare, USA) in a buffer containing
102 40 mM HEPES pH 7.5, 1mM EGTA, 150 mM NaCl, 1 mM MgCl₂ and 5% glycerol.
103 The purified nsp12 was concentrated and stored at 4 °C. Full-length nsp7 (without
104 purification tag) and nsp8 (with a 6 × His-SUMO tag) of SARS-CoV-2 were co-
105 expressed in *E. coli* BL21 (DE3) cells. After purification by Ni-NTA affinity
106 chromatography, the nsp7-nsp8 complex was eluted through on-column tag cleavage
107 by ULP protease and further loaded on a Superdex 200 10/300 Increase column (GE
108 Healthcare, USA) in a buffer containing 40 mM HEPES pH 7.5, 1mM EGTA,150
109 mM NaCl, 1 mM MgCl₂ and 5% glycerol.
110 For the assembly of RdRp, purified nsp12 was incubated with nsp7 and nsp8 at 4 °C
111 for 3 hours at a molar ratio of 1:2:2 in a buffer containing 40 mM HEPES pH 7.5,
112 1mM EGTA, 150 mM NaCl, 1 mM MgCl₂ and 5% glycerol. The stable complex
113 sample was further purified by a Superdex 200 10/300 Increase column (GE

114 Healthcare, USA) in a buffer containing 40 mM HEPES pH 7.5, 1mM EGTA ,150
115 mM NaCl, 1 mM MgCl₂ and 5% glycerol.

116

117 **Protein labeling**

118 All pET28a-N proteins (WT and mutants), nsp12, RdRp complex (nsp12-nsp7-nsp8)
119 and nsp3-Ubl1 proteins were labeled by incubating with a 1:1 molar ratio of Alexa
120 Fluor™ 546 carbox (Thermo Fisher Scientific) for 1 h at room temperature with
121 continuous stirring. Then, the free dyes were removed by centrifugation in
122 MICROSPIN G-50 column (GE Healthcare, 27-5330-01). The labeled proteins were
123 stored at -80°C. For *in vitro* phase separation experiments, 5% labeled protein was
124 mixed with unlabeled before use.

125

126 **Synthesis of RNA and DNA**

127 The 5'-Cy5-labeled 30-bp RNA oligos (viral RNA:
128 GAUUUCAUCUAAACGAACAAACUAAAAUGU; human β actin RNA:
129 UCACCAACUGGGACGACAUGGAGAAAAUCU) were synthesized at
130 HIPPOBIO, LLC. The double-strand RNA was annealed at 25 μM in the annealing
131 buffer (40 mM HEPES, pH 7.4, and 150 mM NaCl) using a thermocycler, during
132 which the oligos were heated up to 95 °C for 2 min and gradually cooled to 25°C over
133 an hour.

134

135 **Phase separation assays**

136 *In vitro* LLPS experiments were performed at room temperature. All samples were
137 seeded and recorded on 384 low-binding multi-well 0.17 mm microscopy plates (In
138 Vitro Scientific) and sealed with optically clear adhesive film. For phase separation
139 assays with the mEGFP-N protein of SARS-CoV-2, solutions of GFP fusion proteins
140 were diluted to the indicated final concentrations in 20 mM HEPES, pH 7.4, 150 mM
141 NaCl, 5% glycerol, 1 mM EGTA and 1mM MgCl₂ in a total volume of 10 μl to

142 induce phase separation. For the N proteins without tags, the assays were performed
143 in 20 mM Tris-HCl, pH 7.5 and 150 mM NaCl. For phase separation assays treated
144 with small molecules, CVL218 or PJ34 (dissolved in 1% DMSO) were added to the
145 well mixed phase separation samples prior to imaging at a final concentration of 20
146 μM . The group treated with 1% DMSO was used as the control.

147 For *in cellulo* assays, Vero E6 cells were seeded into 4-well chamber 35 mm dishes
148 with a density of 5×10^5 cells/well. For cells to reach 70% confluent, 1 μg
149 pCDNA3.1-mcherry-N plasmid was transfected, with the replacement of normal cell
150 culture medium by that supplemented with CVL218 or PJ34 at a final concentration
151 of 20 μM . For the control wells, cell medium containing 1% DMSO was added.

152 Imaging was performed with a NIKON A1 microscope equipped with a 100 \times oil
153 immersion objective. NIS-Elements AR Analysis was used to analyze the images.

154

155 **Fluorescence recovery after photobleaching (FRAP) measurements *in cellulo* and** 156 ***in vitro***

157 FRAP experiments were carried out with a NIKON A1 microscope equipped with a
158 100 \times oil immersion objective. Droplets were bleached with the corresponding laser
159 pulse (3 repeats, 80% intensity, and dwell time 1 s). Recovery from photobleaching
160 was recorded for the indicated time point.

161

162 **Mutation frequency analysis**

163 To perform the mutation frequency analysis of SARS-CoV-2 N protein, we used
164 61,003 SARS-CoV-2 genome sequences downloaded from the China National Center
165 for Bioinformation, 2019 Novel Coronavirus Resource(Zhao et al., 2020)
166 (downloaded on July 6th, 2020). We considered all the missense mutations among the
167 N protein region (from positions 28,274 to 29,530 in the genome).

168

169 **Surface plasmon resonance assays**

170 Surface plasmon resonance (SPR) assays were performed on Biacore S200 with a
171 CM5 sensor chip (GE Healthcare Life Sciences) at room temperature. The full-length
172 N protein, NTD and CTD of SARS-CoV-2 were all diluted in 10 mM sodium acetate
173 (pH 5.0) and immobilized on a CM5 sensor chip by amine coupling. The running
174 buffer contained 1×PBS-P with 2% DMSO. The tested drugs (CVL218 or PJ34) in 2-
175 fold serial dilutions were made in the running buffer. The solutions flowed through
176 the chip surface at a flow rate of 20 μ L/min at room temperature (25°C). The
177 dissociation constants (K_D) of CVL218 and PJ34 binding to full-length N protein,
178 NTD and CTD were calculated from the association and dissociation curves of the
179 sensorgrams using the BIA evaluation program (Biacore).

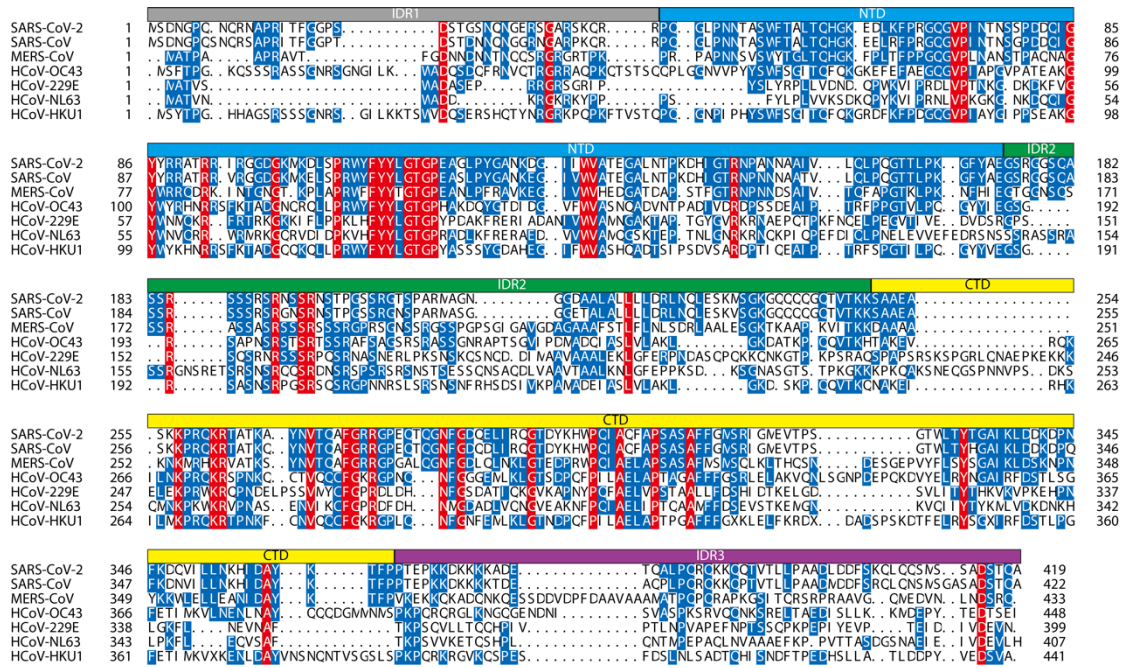
180

181 **Inhibitor combination assay**

182 To assess the potential synergistic effect, CVL218 and remdesivir were mixed with a
183 concentration ratio of 4:1, while CVL218 or remdesivir alone was used as control.
184 The concentration ratios were selected according to the corresponding EC25 values of
185 individual drugs against SARS-CoV-2 *in vitro*. The mixtures were tested for their
186 inhibitory activities against the SARS-CoV-2 with a multiplicity of infection (MOI)
187 of 0.05. Each sample was tested in triplicate.

188

189 **Supplementary Figures**

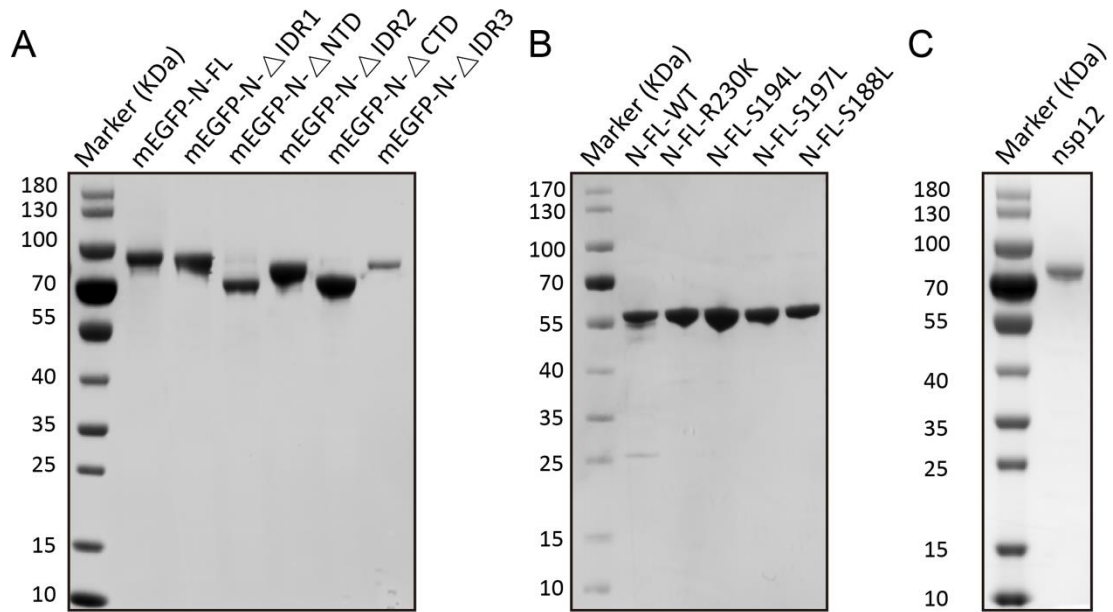


190

191

192 **Figure S1. Multiple sequence alignment of the N proteins from different human**
 193 **coronaviruses.**

194 The nucleocapsid (N) protein sequences of the currently known coronaviruses that can
 195 infect human, including SARS-CoV-2 (GenBank: QHD43423.2), SARS-CoV
 196 (GenBank: AYW99827.1), MERS-CoV (GenBank: AVV62544.1), HCoV-OC43
 197 (GenBank: AAR01019.1), HCoV-229E (GenBank: APD51511.1), HCoV-NL63
 198 (NCBI Reference Sequence: YP_009328939.1) and HCoV-HKU1 (GenBank:
 199 ARU07581.1), were aligned using MUSCLE(38). Domain architectures are depicted
 200 above the sequence alignment. The conserved residues are shaded in red, while those
 201 with the percentage of conservation larger than or equal to 50% are shaded in blue.
 202



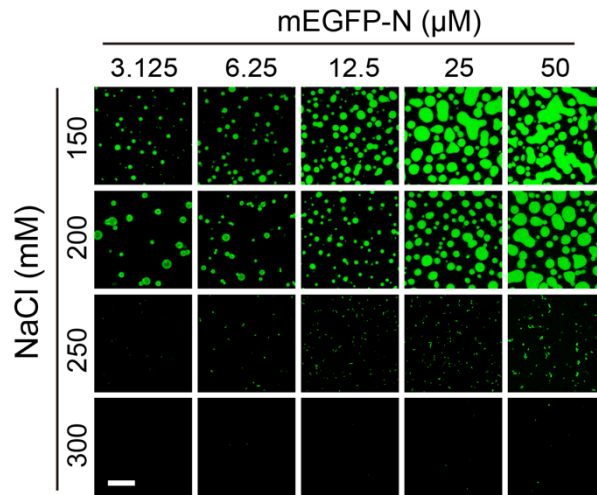
203

204

205 **Figure S2. SDS-PAGE of the purified recombinant proteins of SARS-CoV-2 N and**
 206 **nsp12 used in *in vitro* assays.**

207 (A) The mEGFP-tagged full-length (FL) and truncated proteins of SARS-CoV-2 N. (B)
 208 The wild-type and mutant proteins of SARS-CoV-2 N with His-tagged at the N
 209 terminus. (C) The nsp12 protein of SARS-CoV-2. The gel was stained with Coomassie
 210 Brilliant Blue.

211



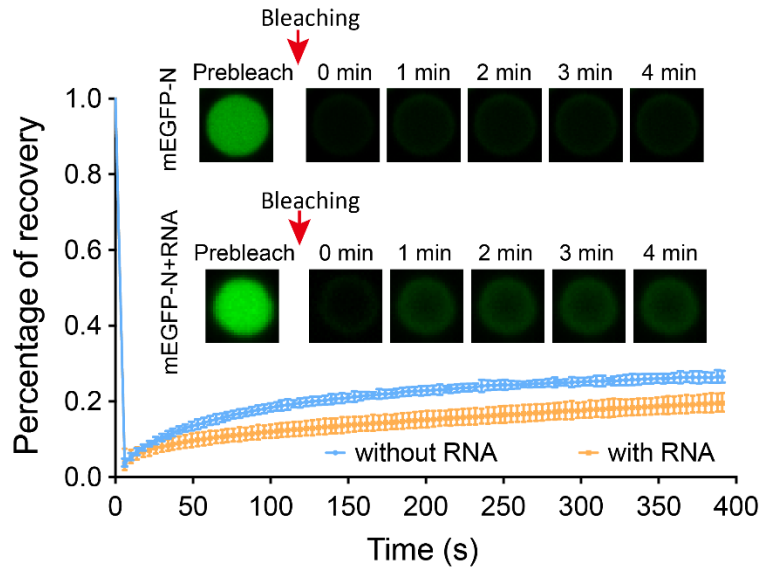
212

213

214 **Figure S3. Phase condensation of SARS-CoV-2 N was sensitive to the increase of**
 215 **ionic strength.**

216 Fluorescence microscopy observations of mEGFP-N condensates *in vitro* depending on
 217 different sodium chloride concentrations and protein concentrations. Scale bar, 20 μm.

218



219

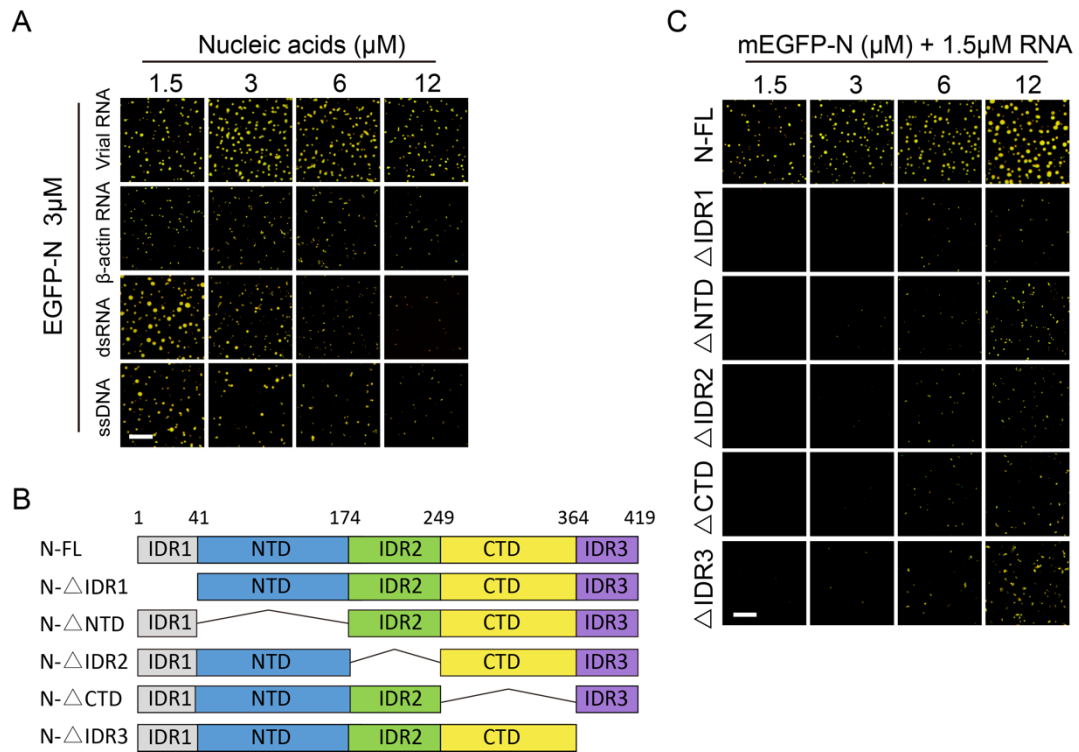
220

221 **Figure S4. *In vitro* FRAP analysis of mEGFP-N condensates (3 μ M) with a**
 222 **complete bleach region.**

223 Top, representative snapshots of condensates before and after bleaching. Bottom,
 224 average fluorescence recovery traces of mEGFP-N condensates. Data are
 225 representative of three independent experiments and presented as mean \pm SD.

226

227



228

229

230 **Figure S5. Phase diagrams of RNA with SARS-CoV-2 N and truncations.**

231 (A) *In vitro* phase separation assays of mEGFP-N with nucleic acids from distinct

232 sources and at different concentrations. Only the merged channel is shown here. Scale

233 bar, 20 μm . (B) Diagram of the structural domains of SARS-CoV-2 N. Truncated

234 proteins for functional analyses of different domains are shown underneath. (C) *In vitro*

235 phase separation assays of full-length (FL) mEGFP-N and truncations with 1.5 μM viral

236 RNA at different concentrations of SARS-CoV-2 N (The numbers under the line

237 represent the concentrations of the proteins). Scale bar, 20 μm .

238

239

240

241

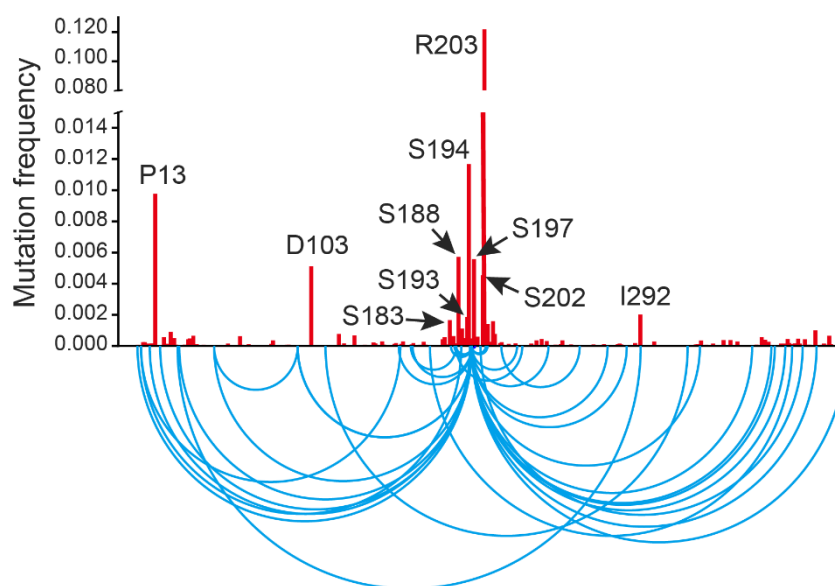
242

243

244

245

246



247

248

249 **Figure S6. Frequencies of spontaneous missense mutations in the N protein in**
250 **61,003 SARS-CoV-2 genome sequences from the China National Center for**
251 **Bioinformatics.**

252 Residue positions of the top 10 most frequent missense mutations are labeled. Bottom,
253 arc diagram of double missense mutations. Only those double missense mutations with
254 frequencies more than 0.0001 are shown.

255

256

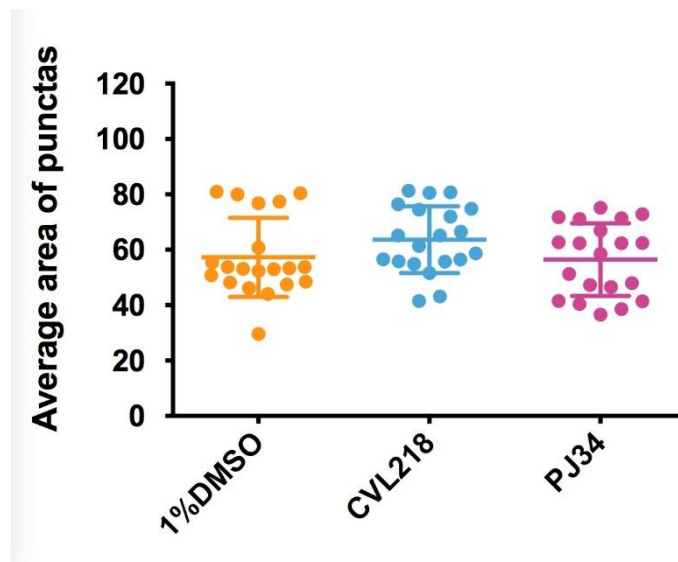
257

258

259

260

261



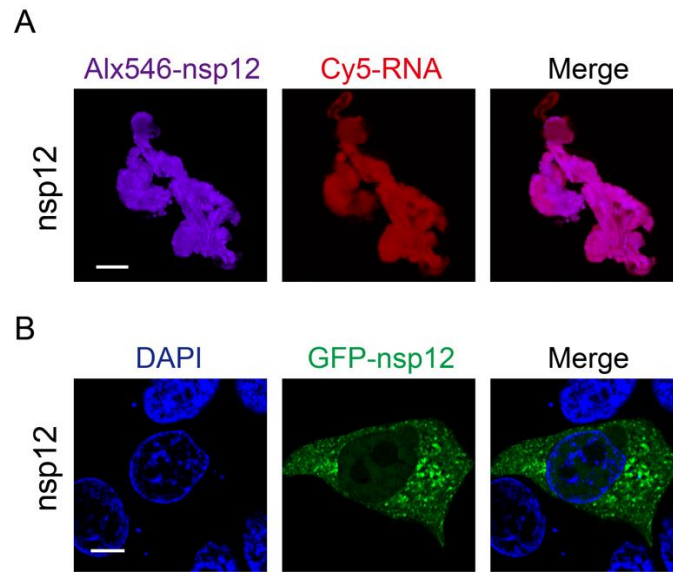
262

263 **Figure S7. Quantitative comparison of the average area of N protein puncta *in***
 264 ***cellulo*.**

265 Total 20 puncta within five Vero E6 cells transfected with mCherry-N were measured
 266 in each treatment to compare the average area of puncta. Data are shown as mean \pm
 267 SD using ImageJ analysis.

268

269



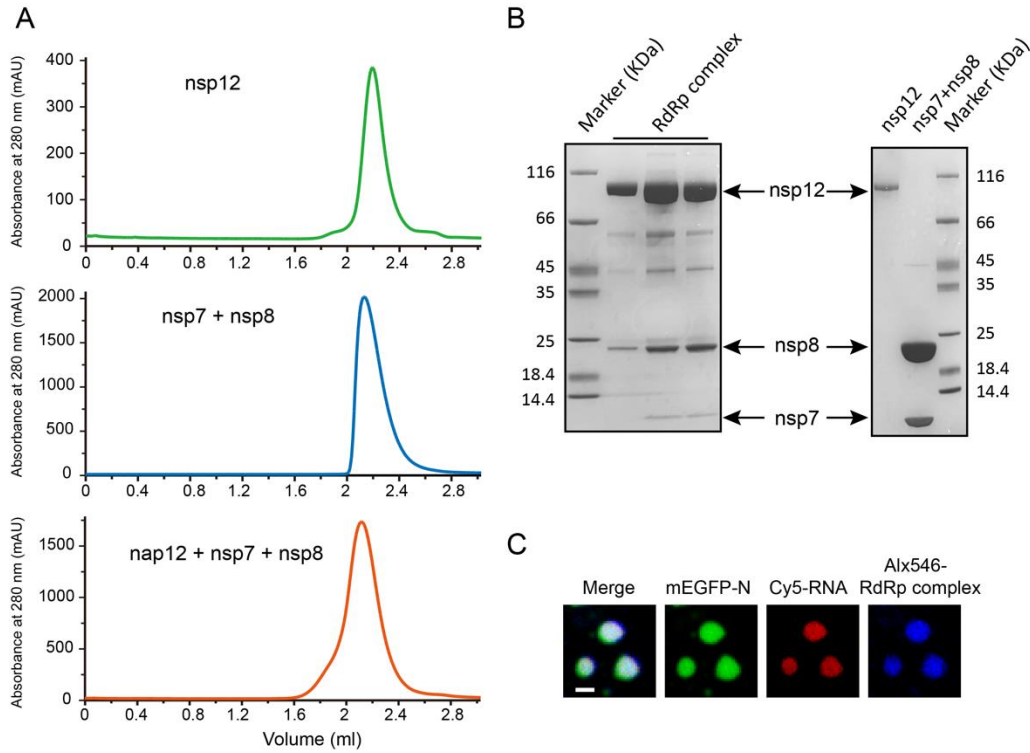
270

271

272 **Figure S8. Nsp12 and viral RNA of SARS-CoV-2 form amorphous condensates *in***
 273 ***vitro*.**

274 **(A)** Fluorescence microscopy images of 3 μ M Alx546-labeled nsp12 (purple) mixed
 275 with 3 μ M Cy5-labeled viral RNA (red) of SARS-CoV-2. Scale bar, 5 μ m. **(B)**
 276 Locations of overexpressed GFP-nsp12 in Vero E6 cells after 48h transfection. The
 277 nuclei were labeled by DAPI. Scale bars, 5 μ m.

278



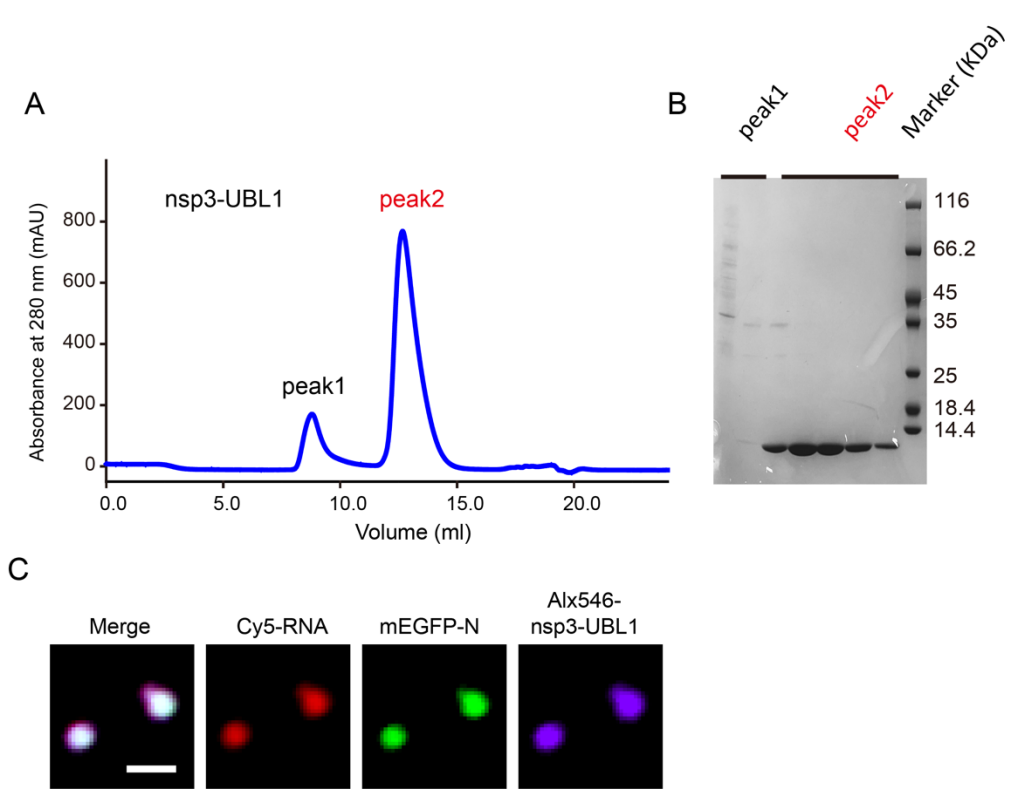
279

280

281 **Figure S9. Purification of SARS-CoV-2 polymerase catalytic complex and its**
 282 **phase separation with the nucleocapsid protein.**

283 (A) Gel filtration chromatography analysis of nsp12, nsp7-nsp8 complex and
 284 assembled RdRp complex (nsp12+nsp7+nsp8) by Superdex 200 Increase 5/150 GL
 285 column. (B) SDS-PAGE analysis of the chromatography peaks according to (A). (C)
 286 *In vitro* phase separation assay for 3 μM mEGFP-N protein with 3 μM Cy5-labeled 30-
 287 nt viral RNA in the presence of 3 μM RdRp complex. Scale bar, 2 μm.

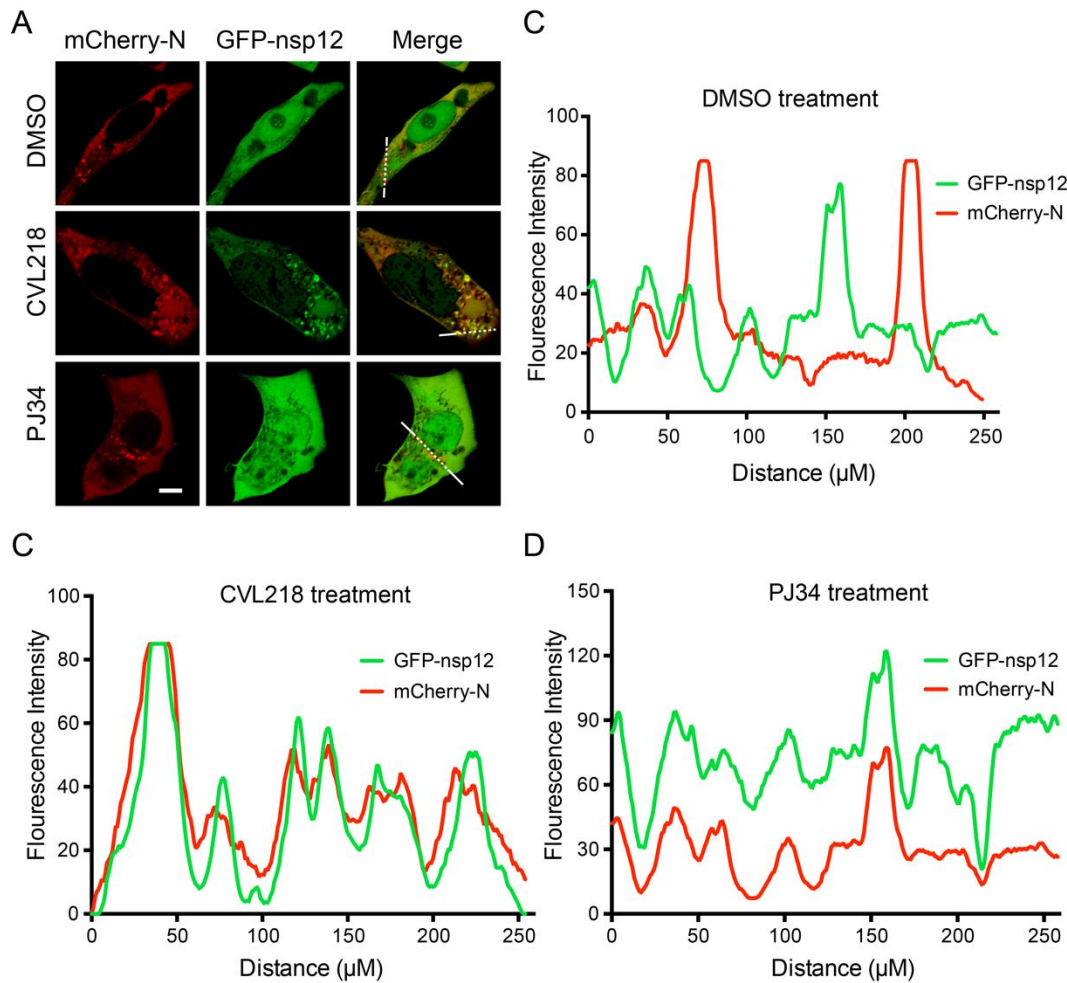
288



289
 290
 291
 292
 293
 294
 295
 296
 297
 298
 299
 300
 301
 302
 303

Figure S10. The Ubl1 domain of SARS-CoV-2 nsp3 can be recruited by nucleocapsid protein *in vitro*.

(A) Gel filtration chromatograph analysis of nsp3-Ubl1 by Superdex 75 Increase 100/300 GL column. (B) SDS-PAGE analysis of the chromatograph peaks corresponding to (A). (C) *In vitro* phase separation assay of 3 μ M mEGFP-N protein with 3 μ M Cy5-labeled 30-nt viral RNA in the presence of 3 μ M nsp3-Ubl1 protein. Scale bar, 2.5 μ m.



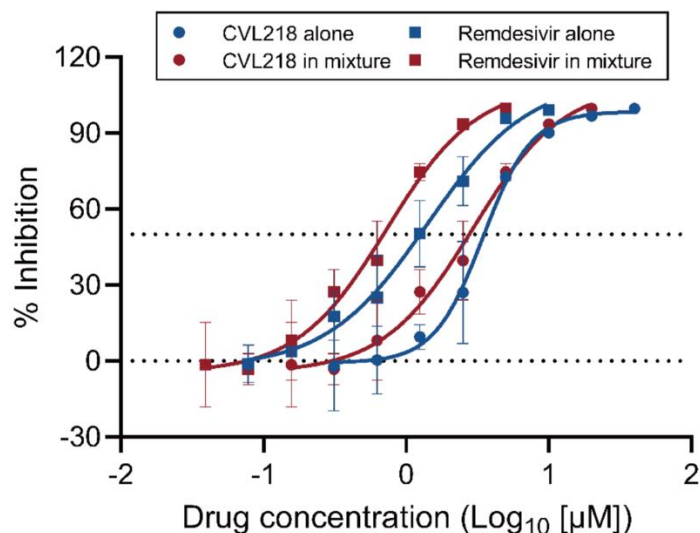
304

305

306 **Figure S11. CVL218/PJ34 treatment enhances the co-localization of SARS-CoV-2**
 307 **N and nsp12 in Vero E6 cells.**

308 (A) Locations of overexpressed GFP-nsp12 (green) and mCherry-N (red) in Vero E6
 309 cells after 48h transfection under three different treatments (DMSO, CVL218 or PJ34,
 310 20 μ M, respectively, 20 μ m). The nucleus was labeled by DAPI. Scale bar, 5 μ m. (B-D)
 311 Co-localization analyses of SARS-CoV-2 N and nsp12 in cells under three different
 312 treatments (DMSO, CVL218 or PJ34, respectively). The fluorescence intensities were
 313 measured along the dotted lines in the merged images shown in (A).

314



315

316

317 **Figure S12. The antiviral activities of the tested drugs against SARS-CoV-2 in**

318 **Vero E6 cells.**

319 Vero E6 cells were infected with SARS-CoV-2 at an MOI of 0.05 in the treatment of

320 different doses of the indicated drugs for 48h. The viral yield in cell supernatant was

321 quantified by qRT-PCR and the results are shown as mean \pm SD over three independent

322 experiments. For the drug combination assays, CVL218 and remdesivir were mixed

323 with a concentration ratio of 4:1. The EC₅₀ values inhibiting the replication of SARS-

324 CoV-2 for remdesivir alone, remdesivir in mixture, CVL218 alone and CVL218 in

325 mixture are 1.41 μ M, 0.73 μ M, 3.46 μ M and 2.93 μ M, respectively.

326

327

328